

# Antenna Coding Optimization for Pixel Antenna Empowered MIMO Wireless Power Transfer

Yijun Chen, *Graduate Student Member, IEEE*, Shanpu Shen, *Senior Member, IEEE*, Tianrui Qiao, *Member, IEEE*, Hongyu Li, *Graduate Student Member, IEEE*, Kai-Kit Wong, *Fellow, IEEE*, and Ross Murch, *Fellow, IEEE*

**Abstract**—We investigate antenna coding utilizing pixel antennas as a new degree of freedom for enhancing multiple-input multiple-output (MIMO) wireless power transfer (WPT) systems. The objective is to enhance the output direct current (DC) power under RF combining and DC combining schemes by jointly exploiting gains from antenna coding, beamforming, and rectenna nonlinearity. We first propose the MIMO WPT system model with binary and continuous antenna coding using the beampoint channel model and formulate the joint antenna coding and beamforming optimization using a nonlinear rectenna model. We propose two efficient closed-form successive convex approximation algorithms to efficiently optimize the beamforming. To further reduce the computational complexity, we propose codebook-based antenna coding designs for output DC power maximization based on K-means clustering. Results show that the proposed pixel antenna empowered MIMO WPT system with binary antenna coding increases output DC power by more than 15 dB compared with conventional systems with fixed antenna configuration. With continuous antenna coding, the performance improves another 6 dB. Moreover, the proposed codebook design outperforms previous designs by up to 40% and shows good performance with reduced computational complexity. Overall, the significant improvement in output DC power verifies the potential of leveraging antenna coding utilizing pixel antennas to enhance WPT systems.

**Index Terms**—Antenna coding, beampoint, beamforming, codebook, DC combining, MIMO, pixel antenna, RF combining, rectenna nonlinearity, wireless power transfer.

## I. INTRODUCTION

WITH the rapid development of wireless sensor networks (WSN) and the Internet of Things (IoT) in the past decades, there has been an explosive increase in devices including wearable devices, RFIDs, and biomedical implants. However, energizing a large number of devices poses a critical challenge, as battery replacement or recharging becomes prohibitive and unsustainable. Wireless power transfer (WPT), where the radio frequency (RF) energy transmitted from

This work was funded by the Hong Kong Research Grants Council for the General Research Fund (GRF) grant 16208124 and the Science and Technology Development Fund, Macau SAR (File/Project no. 001/2024/SKL). (Corresponding author: Shanpu Shen.)

Yijun Chen, Tianrui Qiao, and Ross Murch are with the Department of Electronic and Computer Engineering, The Hong Kong University of Science and Technology, Clear Water Bay, Kowloon, Hong Kong.

Shanpu Shen is with the State Key Laboratory of Internet of Things for Smart City and Department of Electrical and Computer Engineering, University of Macau, Macau, China (e-mail: shanpushen@um.edu.mo).

Hongyu Li is with the Internet of Things Thrust, The Hong Kong University of Science and Technology (Guangzhou), Guangzhou 511400, China.

Kai-Kit Wong is with the Department of Electronic and Electrical Engineering, University College London, Torrington Place, WC1E 7JE, United Kingdom and Yonsei Frontier Lab, Yonsei University, Seoul, Korea.

a dedicated energy transmitter (ET), without any wires, is received and rectified into direct current (DC) energy at an energy receiver (ER), provides a potentially convenient and reliable solution to energize a large number of devices [1].

The main challenge of WPT is to maximize the end-to-end power transfer efficiency, i.e. maximizing the output DC power for a given transmit power. To this end, one approach is efficient rectenna design with enhanced performance in aspects of antenna gain, bandwidth, and impedance matching [2], [3]. In addition, compact multiport rectennas [4], [5], [6], [7] have been developed to maximize the output DC power, but lacks a system-level consideration. Another approach is efficient signal design for WPT, including beamforming, waveform, modulation, and power allocation designs [8], [9]. Previous works [10], [11], [12], [13], [14] have studied the design of multi-sine WPT waveforms that adapt to channel conditions to maximize the output DC power. In [11] and [12], systematic designs of multi-antenna WPT have been proposed, where the beamforming gain, frequency-selectivity and rectenna nonlinearity are jointly leveraged under DC combining and RF combining schemes. Nevertheless, current WPT systems are mainly based on antennas with fixed configuration, while overlooking the potential of reconfigurable antennas to further boost the output DC power.

Pixel antennas are a promising highly reconfigurable antenna technology [15], [16], [17] that can be incorporated into WPT systems to achieve a breakthrough in boosting output DC power. Pixel antennas consist of discretized sub-wavelength elements referred to as pixels, which can be connected together with RF switches. By controlling the states of RF switches, pixel antennas support a wide range of reconfigurability in antenna characteristics such as radiation pattern [16], [17], [18], operating frequency [19], [20], and polarization [21]. Closely related to pixel antennas, there is also an emerging technology (introduced in 2020), termed the fluid antenna system (FAS) [22], [23]. The concept of FAS is based on dynamic adjustment of antenna positions within a linear region to obtain better channel conditions and enhance wireless communication [24], [25]. FAS can be implemented by mechanical movement using liquids or by pixel antennas to mimic the position adjustment through optimizing RF switch configuration [26], [27]. Leveraging the antenna position adjustable property, FAS has been applied to different applications including fluid antenna multiple access (FAMA) [28], wireless powered NOMA systems [29], simultaneous wireless information and power transfer (SWIPT) [30], and FAMA-assisted integrated data and energy transfer [31].

While the development of FAS has demonstrated the benefits of reconfigurable antennas in wireless systems, to further leverage the potential of pixel antennas and generalize the radiation pattern reconfigurability, a novel technology denoted as antenna coding has been recently proposed in [32]. In antenna coding binary variables called antenna coders are utilized to represent the states of RF switches. It has been demonstrated that antenna coding technology can enhance the channel gain of single-input single-output (SISO) systems and the channel capacity of multiple-input multiple-output (MIMO) systems [32]. In addition, it has also been shown to enhance the sum rate in multi-user MISO systems, where pixel antennas are deployed at the user side, through jointly optimizing antenna coding and transmit precoding [33]. Considering the limitation of WPT systems based on antennas with fixed configuration and the significant potential of pixel antennas in designing and enhancing wireless systems, it is useful to investigate pixel antennas with antenna coding optimization in WPT systems. This approach promises to overcome the limitation of low power transfer efficiency in WPT, which remains an open challenging problem.

In this work, we aim to jointly optimize antenna coding with beamforming and combining for pixel antenna MIMO WPT systems to maximize the output DC power. We further broaden and deepen the investigation [34] by considering continuous antenna coding, lower complexity algorithms, RF combining scenarios, and codebook-based antenna coding designs. The contributions of this work are summarized as follows.

*First*, we propose the pixel antenna MIMO WPT system with both binary and continuous antenna coding to greatly enhance the output DC power to overcome the limitation of low power transfer efficiency. To that end, we introduce the MIMO beamspace channel model, which can demonstrate the pattern reconfigurability utilizing pixel antennas and reduce channel estimation overhead in MIMO WPT systems.

*Second*, we formulate and solve the MIMO WPT output DC power maximization problem for DC combining schemes, where the transmit beamforming and antenna coding designs are jointly considered and alternatively optimized. Specifically, to handle the complex non-convex transmit beamforming design, we derive closed-form solutions based on a successive convex approximation (SCA) method, which is more efficient than previous geometric programming with semi-definite relaxation (SDR) methods [11]. We also propose both binary and continuous antenna coding designs, by using Successive Exhaustive Boolean Optimization (SEBO) and the quasi-Newton method, respectively.

*Third*, we formulate and solve the MIMO WPT DC power maximization problem for RF combining schemes. With the alternating optimization approach, we propose both binary and continuous antenna coding designs and closed-form solution for beamforming designs. In particular, we also propose an efficient SCA algorithm for the analog receive beamforming design, which is a practical and low-complexity RF combining scheme by utilizing phase shifters.

*Fourth*, we propose an efficient codebook design based on K-means clustering to reduce the computational complexity of binary antenna coding design, which considers the MIMO

WPT configuration and the objective of output DC power maximization problems. After the offline codebook training, the antenna coder for each pixel antenna is online deployed by searching the codebook.

*Fifth*, we evaluate the average output DC power of the proposed pixel antenna empowered MIMO WPT system with antenna coding. Compared with conventional systems with fixed antenna configuration, using binary antenna coding can significantly enhance the average output DC power by more than 15 dB. Moreover, using continuous antenna coding brings another 6 dB gain compared with binary antenna coding. The proposed codebook-based antenna coding design also outperforms the random codebook and existing design [32] by up to 40%, providing good performance but with much lower computational complexity.

*Organization*: Section II introduces a beamspace channel model and MIMO WPT system model with binary and continuous antenna coding. Section III presents the joint antenna coding and beamforming design with DC combining scheme. Section IV presents the joint antenna coding and beamforming design with RF combining scheme. Section V presents the codebook-based antenna coding design. Section VI provides performance evaluations for the proposed pixel antenna empowered MIMO WPT system. Section VII concludes this work.

*Notation*: Bold lowercase and uppercase letters represent vectors and matrices, respectively. A symbol without bold font denotes a scalar.  $\mathcal{E}\{\cdot\}$ ,  $\Re\{\cdot\}$ ,  $\mathbb{R}$  and  $\mathbb{C}$  represent expectation, real part, real and complex number sets, respectively.  $[\mathbf{a}]_i$ ,  $\mathbf{a}^*$ , and  $\|\mathbf{a}\|$  denote the  $i$ th element, conjugate, and  $l_2$ -norm of a vector  $\mathbf{a}$ , respectively.  $\mathbf{A}^T$ ,  $\mathbf{A}^H$ ,  $[\mathbf{A}]_{i,:}$ ,  $[\mathbf{A}]_{:,i}$ , and  $[\mathbf{A}]_{i,j}$  denote the transpose, conjugate transpose,  $i$ th row,  $i$ th column, and  $(i, j)$ th element of a matrix  $\mathbf{A}$ , respectively.  $\cup$  denotes the union of sets.  $\mathcal{CN}(\mathbf{0}, \Sigma)$  represents the circularly symmetric complex Gaussian distribution with zero mean and covariance matrix  $\Sigma$ .  $\text{diag}(a_1, \dots, a_N)$  denotes a diagonal matrix with entries  $a_1, \dots, a_N$ .  $\text{blkdiag}(\mathbf{a}_1, \dots, \mathbf{a}_N)$  denotes a block diagonal matrix formed by  $\mathbf{a}_1, \dots, \mathbf{a}_N$ .  $j$  is the imaginary unit.  $\mathbf{I}$  denotes the identity matrix.

## II. MIMO WPT SYSTEM UTILIZING PIXEL ANTENNAS

The basic principle of MIMO WPT systems utilizing pixel antennas is introduced in this section, including the concept of antenna coding, beamspace channel model, and MIMO WPT system model.

### A. Pixel Antennas and Antenna Coding

We first briefly introduce the pixel antenna model and the corresponding antenna coding technology. As shown in Fig. 1(a), the pixel antenna is based on a discretized radiation surface consisting of sub-wavelength pixels. Adjacent pixels are connected through  $Q$  RF switches or variable reactive loads, which can be flexibly adjusted to reconfigure the antenna characteristics. According to multiport network theory [20], the pixel antenna can be accurately modeled as a  $(Q + 1)$ -port network with one antenna port and  $Q$  pixel ports as shown in Fig. 1(b). We characterize the  $(Q + 1)$ -port

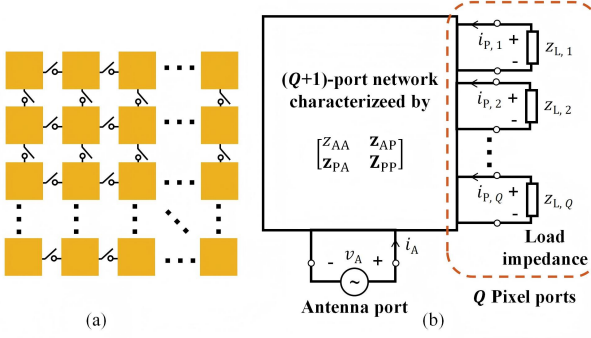


Fig. 1. Schematics of (a) pixel antenna and (b) multiport network model.

network by its impedance matrix  $\mathbf{Z} = [z_{AA}, \mathbf{z}_{AP}; \mathbf{z}_{PA}, \mathbf{Z}_{PP}] \in \mathbb{C}^{(Q+1) \times (Q+1)}$ , where  $z_{AA} \in \mathbb{C}$  and  $\mathbf{Z}_{PP} \in \mathbb{C}^{Q \times Q}$  denote the self-impedance (matrix) for the antenna port and pixel ports respectively,  $\mathbf{z}_{AP} \in \mathbb{C}^{1 \times Q}$  and  $\mathbf{z}_{PA} \in \mathbb{C}^{Q \times 1}$  represent the trans-impedance between the antenna port and pixel ports with  $\mathbf{z}_{AP} = \mathbf{z}_{PA}^T$ . The voltages and currents of the  $(Q+1)$ -port network are therefore related by

$$\begin{bmatrix} v_A \\ \mathbf{v}_P \end{bmatrix} = \begin{bmatrix} z_{AA} & \mathbf{z}_{AP} \\ \mathbf{z}_{PA} & \mathbf{Z}_{PP} \end{bmatrix} \begin{bmatrix} i_A \\ \mathbf{i}_P \end{bmatrix}, \quad (1)$$

where  $v_A \in \mathbb{C}$  and  $\mathbf{v}_P = [v_{P,1}, \dots, v_{P,Q}]^T \in \mathbb{C}^{Q \times 1}$  denote the voltages at the antenna port and pixel ports, and the currents at the antenna port and pixel ports are  $i_A \in \mathbb{C}$  and  $\mathbf{i}_P = [i_{P,1}, \dots, i_{P,Q}]^T \in \mathbb{C}^{Q \times 1}$ , respectively.

Depending on whether adjacent pixels are connected by either RF switches or variable reactive loads, we achieve binary antenna coding or continuous antenna coding, as detailed below.

1) *Binary Antenna Coding*: Leveraging RF switches, adjacent pixels in the pixel antenna can be reconfigured to be either connected or unconnected. This enables the antenna topology to be reconfigured to create the desired antenna characteristics. Accordingly, the  $q$ th RF switch can be modeled as load impedance  $z_{L,q} \in \mathbb{C}$ , which is either short-circuit or open-circuit depending on the switch on (connected) or off (unconnected) state. Therefore, we can use a binary variable  $b_q \in \{0, 1\}$  to characterize the switch state, i.e.  $b_q = 0$  for switch on state and  $b_q = 1$  for switch off state, so that we have

$$z_{L,q} = \begin{cases} 0, & \text{if } b_q = 0, \\ \infty, & \text{if } b_q = 1, \end{cases} \quad (2)$$

where the infinity for the switch off state, i.e. the open-circuit load impedance, can be numerically approximated by a very large value  $jx_{oc}$ , e.g.  $x_{oc} = 10^9$ . Thus, we can rewrite (2) as

$$z_{L,q} = jx_{oc}b_q. \quad (3)$$

We collect  $b_q \forall q$  into a vector  $\mathbf{b} = [b_1, \dots, b_Q]^T \in \mathbb{R}^{Q \times 1}$  to denote all switch states, which is denoted here as the antenna coder.

2) *Continuous Antenna Coding*: To enhance the reconfigurability of the pixel antenna, we can extend the binary antenna coding to continuous antenna coding by replacing the

RF switches with variable reactive loads such as varactors. Similarly, the  $q$ th variable reactive load can be modeled as load impedance  $z_{L,q}$ , written as

$$z_{L,q} = jx_{L,q}, \quad (4)$$

where  $x_{L,q} \in \mathbb{R}$  is the load reactance for the  $q$ th variable reactive load. The load reactance  $x_{L,q}$  can be positive/negative infinity in theory, while numerically it can be expressed as

$$|x_{L,q}| = x_{oc}b_q, \quad b_q \in [0, 1], \quad (5)$$

where the antenna coder  $b_q \forall q$  can be continuous in the range  $[0, 1]$  and the binary antenna coding with the open/short-circuit load impedance (3) is a special case.

For both binary and continuous antenna coding, we can group  $z_{L,q} \forall q$  into a diagonal load impedance matrix  $\mathbf{Z}_L(\mathbf{b}) = \text{diag}(z_{L,1}, \dots, z_{L,Q}) \in \mathbb{C}^{Q \times Q}$ , which is coded by  $\mathbf{b}$ , so that  $\mathbf{v}_P$  and  $\mathbf{i}_P$  can be related by

$$\mathbf{v}_P = -\mathbf{Z}_L(\mathbf{b})\mathbf{i}_P. \quad (6)$$

Substituting (6) into (1), we can obtain the currents at pixel ports  $\mathbf{i}_P(\mathbf{b})$  with excitation  $i_A$  as

$$\mathbf{i}_P(\mathbf{b}) = -(\mathbf{Z}_{PP} + \mathbf{Z}_L(\mathbf{b}))^{-1}\mathbf{z}_{PA}i_A. \quad (7)$$

We collect the currents at all ports into a vector  $\mathbf{i}(\mathbf{b}) = [i_A; \mathbf{i}_P(\mathbf{b})] \in \mathbb{C}^{(Q+1) \times 1}$ .

The radiation pattern  $\mathbf{e}(\mathbf{b}) \in \mathbb{C}^{2K \times 1}$  generated by the pixel antenna is given by

$$\mathbf{e}(\mathbf{b}) = \mathbf{e}_A i_A + \sum_{q=1}^Q \mathbf{e}_{P,q} i_{P,q}(\mathbf{b}) = \mathbf{E}_{oc} \mathbf{i}(\mathbf{b}), \quad (8)$$

where  $\mathbf{e}_A \in \mathbb{C}^{2K \times 1}$  and  $\mathbf{e}_{P,q} \in \mathbb{C}^{2K \times 1}$  are the radiation patterns of the antenna port and  $q$ th pixel port (with  $\theta$  and  $\phi$  polarization components over  $K$  sampled spatial angles) excited by unit current when other ports are open-circuit, respectively, and  $\mathbf{E}_{oc} = [\mathbf{e}_A, \mathbf{e}_{P,1}, \dots, \mathbf{e}_{P,Q}] \in \mathbb{C}^{2K \times (Q+1)}$  is the open-circuit radiation pattern matrix for all ports. For the binary and continuous antenna coding cases, the antenna coders are optimized among  $2^Q$  discrete combinations and in a continuous space, respectively. With the optimized antenna coders, the antenna characteristics such as radiation patterns can be flexibly reconfigured to adapt to the channel, providing extra degrees of freedom to design and enhance WPT systems.

## B. MIMO Beamspace Channel Model

We consider a MIMO pixel antenna system with  $M$  pixel antennas at the transmitter (each coded by  $\mathbf{b}_{T,m}, m = 1, 2, \dots, M$ ) and  $N$  pixel antennas at the receiver (each coded by  $\mathbf{b}_{R,n}, n = 1, 2, \dots, N$ ) as shown in Fig. 2 and Fig. 3, where we assume all pixel antennas are identical and spatially separated. Given the currents of the transmit and receive pixel antennas,  $\mathbf{i}_{T,m}(\mathbf{b}_{T,m}) \in \mathbb{C}^{(Q+1) \times 1} \forall m$  and  $\mathbf{i}_{R,n}(\mathbf{b}_{R,n}) \in \mathbb{C}^{(Q+1) \times 1} \forall n$ , the radiation pattern of each transmit and receive pixel antenna can be respectively written as

$$\mathbf{e}_{T,m}(\mathbf{b}_{T,m}) = \mathbf{E}_{oc,T,m} \mathbf{i}_{T,m}(\mathbf{b}_{T,m}), \quad (9)$$

$$\mathbf{e}_{R,n}(\mathbf{b}_{R,n}) = \mathbf{E}_{oc,R,n} \mathbf{i}_{R,n}(\mathbf{b}_{R,n}), \quad (10)$$

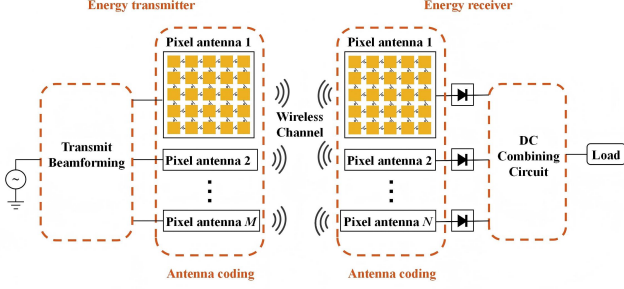


Fig. 2. Schematic of the proposed MIMO WPT system using pixel antennas with DC combining.

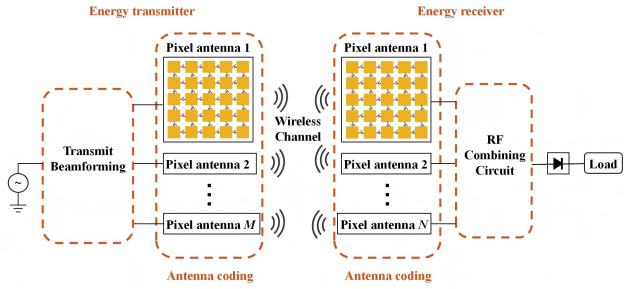


Fig. 3. Schematic of the proposed MIMO WPT system using pixel antennas with RF combining.

where  $\mathbf{E}_{\text{oc},\text{T},m} \in \mathbb{C}^{2K \times (Q+1)}$  and  $\mathbf{E}_{\text{oc},\text{R},n} \in \mathbb{C}^{2K \times (Q+1)}$  are the open-circuit radiation pattern matrices of the  $m$ th transmit and  $n$ th receive pixel antenna, respectively.

Using the beamspace channel representation [35], the channel for the MIMO pixel antenna system can be written as

$$\mathbf{H}(\mathbf{B}_T, \mathbf{B}_R) = \mathbf{E}_R^T(\mathbf{B}_R) \mathbf{H}_V \mathbf{E}_T(\mathbf{B}_T), \quad (11)$$

where  $\mathbf{E}_T(\mathbf{B}_T) = [\mathbf{e}_{T,1}(\mathbf{b}_{T,1}), \dots, \mathbf{e}_{T,M}(\mathbf{b}_{T,M})] \in \mathbb{C}^{2K \times M}$  and  $\mathbf{E}_R(\mathbf{B}_R) = [\mathbf{e}_{R,1}(\mathbf{b}_{R,1}), \dots, \mathbf{e}_{R,N}(\mathbf{b}_{R,N})] \in \mathbb{C}^{2K \times N}$  collect normalized radiation patterns where  $\|\mathbf{e}_{T,m}(\mathbf{b}_{T,m})\| = 1 \forall m$  and  $\|\mathbf{e}_{R,n}(\mathbf{b}_{R,n})\| = 1 \forall n$  are for channel normalization,  $\mathbf{B}_T = [\mathbf{b}_{T,1}, \dots, \mathbf{b}_{T,M}] \in \mathbb{R}^{Q \times M}$  and  $\mathbf{B}_R = [\mathbf{b}_{R,1}, \dots, \mathbf{b}_{R,N}] \in \mathbb{R}^{Q \times N}$  are antenna coder matrices for transmit and receive pixel antennas respectively, and  $\mathbf{H}_V \in \mathbb{C}^{2K \times 2K}$  is the virtual channel matrix collecting channel gains between all pairs of angle of departure (AoD) and angle of arrival (AoA) among the dual polarizations and  $K$  sampled spatial angles.

To demonstrate the additional degrees of freedom provided by pixel antennas, we first perform singular value decomposition (SVD) of the open-circuit radiation pattern matrices  $\mathbf{E}_{\text{oc},\text{T},m} \forall m$  and  $\mathbf{E}_{\text{oc},\text{R},n} \forall n$  of all the transmit and receive pixel antennas. We assume that all pixel antennas are identical, so that the open-circuit radiation patterns of different pixel antennas have the same shape. Thus,  $\mathbf{E}_{\text{oc},\text{T},m} \forall m$  and  $\mathbf{E}_{\text{oc},\text{R},n} \forall n$  share the same rank, which can be denoted as  $N_{\text{eff}}$ . Specifically, using SVD, we have that

$$\mathbf{E}_{\text{oc},\text{T},m} = \mathbf{U}_{\text{T},m} \mathbf{S}_{\text{T},m} \mathbf{V}_{\text{T},m}^H, \quad (12)$$

$$\mathbf{E}_{\text{oc},\text{R},n} = \mathbf{U}_{\text{R},n} \mathbf{S}_{\text{R},n} \mathbf{V}_{\text{R},n}^H, \quad (13)$$

where  $\mathbf{S}_{\text{T},m}, \mathbf{S}_{\text{R},n} \in \mathbb{R}^{N_{\text{eff}} \times N_{\text{eff}}}$  are diagonal matrices containing  $N_{\text{eff}}$  non-zero singular values,  $\mathbf{U}_{\text{T},m} \in \mathbb{C}^{2K \times N_{\text{eff}}}$ ,  $\mathbf{U}_{\text{R},n} \in \mathbb{C}^{2K \times N_{\text{eff}}}$ ,  $\mathbf{V}_{\text{T},m} \in \mathbb{C}^{(Q+1) \times N_{\text{eff}}}$ , and  $\mathbf{V}_{\text{R},n} \in \mathbb{C}^{(Q+1) \times N_{\text{eff}}}$  are semi-unitary matrices of the  $m$ th transmit and  $n$ th receive pixel antenna respectively.  $N_{\text{eff}}$  is also referred to as the effective aerial degrees-of-freedom (EADoF) [36], which indicates the number of orthogonal radiation patterns the pixel antenna can provide. The  $N_{\text{eff}}$  columns of each  $\mathbf{U}_{\text{T},m} \forall m$  and  $\mathbf{U}_{\text{R},n} \forall n$  can be utilized as the orthogonal basis patterns to construct the beamspace. Therefore, the MIMO pixel antenna system can be equivalently viewed as a conventional MIMO system with  $N_{\text{T}} = MN_{\text{eff}}$  and  $N_{\text{R}} = NN_{\text{eff}}$  spatially separated transmit and receive antennas.

Accordingly, we can define the pattern coders for each transmit and receive pixel antennas as

$$\mathbf{w}_{\text{T},m}(\mathbf{b}_{\text{T},m}) = \mathbf{S}_{\text{T},m} \mathbf{V}_{\text{T},m}^H \mathbf{i}_{\text{T},m}(\mathbf{b}_{\text{T},m}), \quad (14)$$

$$\mathbf{w}_{\text{R},n}(\mathbf{b}_{\text{R},n}) = \mathbf{S}_{\text{R},n} \mathbf{V}_{\text{R},n}^T \mathbf{i}_{\text{R},n}^*(\mathbf{b}_{\text{R},n}), \quad (15)$$

which satisfy  $\|\mathbf{w}_{\text{T},m}(\mathbf{b}_{\text{T},m})\| = 1$  and  $\|\mathbf{w}_{\text{R},n}(\mathbf{b}_{\text{R},n})\| = 1$ . With the pattern coder, we can rewrite the radiation pattern of the  $m$ th transmit and  $n$ th receive pixel antenna as

$$\mathbf{e}_{\text{T},m}(\mathbf{b}_{\text{T},m}) = \mathbf{U}_{\text{T},m} \mathbf{w}_{\text{T},m}(\mathbf{b}_{\text{T},m}), \quad (16)$$

$$\mathbf{e}_{\text{R},n}(\mathbf{b}_{\text{R},n}) = \mathbf{U}_{\text{R},n} \mathbf{w}_{\text{R},n}^*(\mathbf{b}_{\text{R},n}), \quad (17)$$

which implies that the radiation pattern of the pixel antenna can be synthesized by linearly coding the orthogonal basis patterns with a pattern coder. Based on (14) and (15), the overall transmit and receive pattern coders are given as block-diagonal matrices  $\mathbf{W}_T(\mathbf{B}_T) = \text{blkdiag}(\mathbf{w}_{\text{T},1}(\mathbf{b}_{\text{T},1}), \dots, \mathbf{w}_{\text{T},M}(\mathbf{b}_{\text{T},M})) \in \mathbb{C}^{N_{\text{T}} \times M}$  and  $\mathbf{W}_R(\mathbf{B}_R) = \text{blkdiag}(\mathbf{w}_{\text{R},1}(\mathbf{b}_{\text{R},1}), \dots, \mathbf{w}_{\text{R},N}(\mathbf{b}_{\text{R},N})) \in \mathbb{C}^{N_{\text{R}} \times N}$ . Utilizing the pattern coder definition to substitute (11), an equivalent beamspace channel model can be written as

$$\mathbf{H}(\mathbf{B}_T, \mathbf{B}_R) = \mathbf{W}_R^H(\mathbf{B}_R) \mathbf{H}_C \mathbf{W}_T(\mathbf{B}_T), \quad (18)$$

where  $\mathbf{H}_C \in \mathbb{C}^{N_{\text{R}} \times N_{\text{T}}}$  denotes the channel between the  $N_{\text{T}}$  and  $N_{\text{R}}$  equivalent spatially separated antennas, written as

$$\mathbf{H}_C = \mathbf{E}_{\text{bs},\text{R}}^T \mathbf{H}_V \mathbf{E}_{\text{bs},\text{T}}, \quad (19)$$

where  $\mathbf{E}_{\text{bs},\text{T}} = [\mathbf{U}_{\text{T},1}, \dots, \mathbf{U}_{\text{T},M}] \in \mathbb{C}^{2K \times N_{\text{T}}}$  and  $\mathbf{E}_{\text{bs},\text{R}} = [\mathbf{U}_{\text{R},1}, \dots, \mathbf{U}_{\text{R},N}] \in \mathbb{C}^{2K \times N_{\text{R}}}$  collect the orthogonal basis patterns of spatially separated transmit and receive pixel antennas, respectively. The formulation (19) has the benefits of reducing channel estimation overhead and optimization complexity as  $\mathbf{H}_C$  has a lower dimension than the virtual channel matrix  $\mathbf{H}_V$ . Considering a rich scattering propagation environment with Rayleigh fading, we can model  $[\mathbf{H}_C]_{i,j} \sim \mathcal{CN}(0, 1) \forall i, j$  as independent and identically distributed (i.i.d.) complex Gaussian random variables, which is consistent with the conventional  $N_{\text{R}} \times N_{\text{T}}$  MIMO Rayleigh channel.

### C. MIMO WPT System Model

For the proposed MIMO WPT system consisting of  $M$  transmit pixel antennas and  $N$  receive pixel antennas, we denote the transmit beamformer as  $\mathbf{p}_T = [p_{\text{T},1}, \dots, p_{\text{T},M}]^T \in \mathbb{C}^{M \times 1}$ , where  $p_{\text{T},m} \forall m$  is the beamforming weight at the  $m$ th

transmit pixel antenna, and it satisfies the power constraint  $\frac{1}{2} \|\mathbf{p}_T\|^2 \leq P$ , where  $P$  is the transmit power. Accordingly, the transmit signal  $\mathbf{x}(t) \in \mathbb{C}^{M \times 1}$  at time  $t$  with transmit beamforming can be written as

$$\mathbf{x}(t) = \Re\{\mathbf{p}_T e^{j\omega_c t}\}, \quad (20)$$

where  $\omega_c$  is the center frequency. The transmit signal then propagates through the beampoint channel  $\mathbf{H}(\mathbf{B}_T, \mathbf{B}_R)$ . Using (18), the received signal  $\mathbf{y}(t) \in \mathbb{C}^{N \times 1}$  can be expressed as

$$\mathbf{y}(t) = \Re\{\mathbf{W}_R^H(\mathbf{B}_R)\mathbf{H}_C\mathbf{W}_T(\mathbf{B}_T)\mathbf{p}_T e^{j\omega_c t}\}. \quad (21)$$

We assume the channel matrix  $\mathbf{H}_C$  is perfectly known to the transmitter and receiver for subsequent antenna coding and beamforming optimization. The CSI can be accurately acquired by channel estimation based on beampoint pilot transmission and feedback [37].

### III. ANTENNA CODING OPTIMIZATION FOR MIMO WPT WITH DC COMBINING

In this section, we formulate and solve the antenna coding optimization problem for MIMO WPT with DC combining (DCC) to maximize the output DC power. An efficient algorithm to jointly optimize antenna coding and transmit beamforming is also proposed.

For DCC scheme, as shown in Fig. 2, the received signal at each receive pixel antenna is individually rectified. We consider a nonlinear rectenna model in [10], [13], so that the output DC voltage of the  $n$ th rectifier is given by

$$v_{\text{out},n} = \sum_{i \text{ even}, i \geq 2}^{n_0} \beta_i \mathcal{E}\{y_n(t)^i\}, \quad (22)$$

where  $n_0$  is the truncation order, e.g.  $n_0 = 4$ ,  $\beta_i = \frac{R_{\text{ant}}^{i/2}}{i!(I_d v_t)^{i-1}}$  is a constant with  $R_{\text{ant}}$ ,  $v_t$ , and  $I_d$  denoting the antenna impedance, thermal voltage, and ideality factor, respectively, and  $\mathcal{E}\{y_n(t)^i\}$  is given by

$$\mathcal{E}\{y_n(t)^i\} = \zeta_i \|\mathbf{H}(\mathbf{B}_T, \mathbf{B}_R)\mathbf{p}_T\|_n^i, \quad (23)$$

where  $\zeta_i = \frac{1}{2\pi} \int_0^{2\pi} \sin^i t dt$  and specifically  $\zeta_2 = \frac{1}{2}$ , and  $\zeta_4 = \frac{3}{8}$ . The individually rectified DC power is then combined using circuits such as a MIMO switching DC-DC converter [38], which yields the output DC power

$$P_{\text{out}}^{\text{DCC}}(\mathbf{p}_T, \mathbf{B}_T, \mathbf{B}_R) = \sum_{n=1}^N \frac{v_{\text{out},n}^2}{R_L}, \quad (24)$$

where  $R_L$  denotes the load impedance of each rectifier.

#### A. Binary Antenna Coding Optimization with DCC

Based on the nonlinear rectenna model, we aim to jointly optimize binary antenna coding and transmit beamforming designs for maximizing the output DC power,

$$\max_{\mathbf{p}_T, \mathbf{B}_T, \mathbf{B}_R} P_{\text{out}}^{\text{DCC}}(\mathbf{p}_T, \mathbf{B}_T, \mathbf{B}_R) \quad (25)$$

$$\text{s.t. } \frac{1}{2} \|\mathbf{p}_T\|^2 \leq P, \quad (26)$$

$$[\mathbf{B}_T]_{i,j} \in \{0, 1\}, \forall i, j, \quad (27)$$

$$[\mathbf{B}_R]_{i,j} \in \{0, 1\}, \forall i, j, \quad (28)$$

where the explicit expression for the objective,  $P_{\text{out}}^{\text{DCC}}(\mathbf{p}_T, \mathbf{B}_T, \mathbf{B}_R)$ , with regard to  $\mathbf{p}_T$ ,  $\mathbf{B}_T$ , and  $\mathbf{B}_R$  can be found by (7), (14), (15), (22), (23), and (24).

As the problem has multiple variables which are highly coupled, we adopt an alternating optimization approach to decompose it into two sub-problems including transmit beamforming and binary antenna coding designs.

1) *Transmit Beamforming Design*: Given fixed antenna coders  $\mathbf{B}_T$  and  $\mathbf{B}_R$ , the channel  $\mathbf{H}(\mathbf{B}_T, \mathbf{B}_R)$  is fixed and  $P_{\text{out}}^{\text{DCC}}$  is solely the function of transmit beamformer  $\mathbf{p}_T$ , so that we can equivalently transform problem (25)-(28) into

$$\max_{\mathbf{p}_T} P_{\text{out}}^{\text{DCC}}(\mathbf{p}_T) \quad (29)$$

$$\text{s.t. } \frac{1}{2} \|\mathbf{p}_T\|^2 \leq P, \quad (30)$$

which is non-convex. Previous works have utilized quasi-Newton [34] or semidefinite relaxation (SDR) methods [11] to solve the problem (29) and (30), but with high complexity. To address this limitation, in this work we propose a computationally efficient algorithm based on successive convex approximation (SCA). Specifically, we introduce auxiliary variables  $r_n = |\mathbf{h}_n \mathbf{p}_T|^2 \forall n$ , where  $\mathbf{h}_n = [\mathbf{H}(\mathbf{B}_T, \mathbf{B}_R)]_{n,:}$  and  $r_n > 0$ . According to (22)-(24), the output DC power with DCC in (29) can be equivalently rewritten as

$$P_{\text{out}}^{\text{DCC}} = \frac{1}{R_L} \sum_{n=1}^N \left( \sum_{i \text{ even}, i \geq 2}^{n_0} \sum_{j \text{ even}, j \geq 2}^{n_0} \beta_i \beta_j \zeta_i \zeta_j r_n^{\frac{i+j}{2}} \right). \quad (31)$$

At the  $k$ th iteration, using the first-order Taylor expansion, we can approximate  $r_n^{\frac{i+j}{2}}$  by

$$r_n^{\frac{i+j}{2}} \geq \frac{i+j}{2} \left( r_n^{(k-1)} \right)^{\frac{i+j}{2}-1} r_n - \frac{i+j-2}{2} \left( r_n^{(k-1)} \right)^{\frac{i+j}{2}}, \quad (32)$$

where  $r_n^{(k-1)}$  is the value of  $r_n$  optimized at the  $(k-1)$ th iteration and is given by  $r_n^{(k-1)} = \mathbf{p}_T^{(k-1)H} \mathbf{h}_n^H \mathbf{h}_n \mathbf{p}_T^{(k-1)}$ . Moreover,  $r_n$  can be approximated by

$$r_n = \mathbf{p}_T^H \mathbf{h}_n^H \mathbf{h}_n \mathbf{p}_T \geq 2\Re\left\{ \mathbf{p}_T^{(k-1)H} \mathbf{h}_n^H \mathbf{h}_n \mathbf{p}_T \right\} - r_n^{(k-1)}, \quad (33)$$

where  $\mathbf{p}_T^{(k-1)}$  is the value of  $\mathbf{p}_T$  optimized at the  $(k-1)$ th iteration. Substituting (33) into (32) yields

$$\begin{aligned} r_n^{\frac{i+j}{2}} &\geq \Re\left\{ (i+j) \left( r_n^{(k-1)} \right)^{\frac{i+j}{2}-1} \mathbf{p}_T^{(k-1)H} \mathbf{h}_n^H \mathbf{h}_n \mathbf{p}_T \right\} \\ &\quad - (i+j-1) \left( r_n^{(k-1)} \right)^{\frac{i+j}{2}}. \end{aligned} \quad (34)$$

Leveraging the approximation in (34) and ignoring the constant term, we can equivalently write the approximate problem at the  $k$ th iteration as

$$\max_{\mathbf{p}_T} \Re\left\{ \mathbf{a}^{(k-1)H} \mathbf{p}_T \right\} \quad (35)$$

$$\text{s.t. } \frac{1}{2} \|\mathbf{p}_T\|^2 \leq P, \quad (36)$$

where  $\mathbf{a}^{(k-1)}$  is a constant given by (35). Utilizing the Cauchy-Schwartz inequality

$$\Re\left\{ \mathbf{a}^{(k-1)H} \mathbf{p}_T \right\} \leq \left| \mathbf{a}^{(k-1)H} \mathbf{p}_T \right| \leq \|\mathbf{a}^{(k-1)}\| \|\mathbf{p}_T\|, \quad (37)$$

$$\mathbf{a}^{(k-1)} = \frac{1}{R_L} \left( \sum_{n=1}^N \sum_{i \text{ even}, i \geq 2}^{n_0} \sum_{j \text{ even}, j \geq 2}^{n_0} \beta_i \beta_j \zeta_i \zeta_j (i+j) [r_n^{(k-1)}]^{\frac{i+j}{2}-1} \mathbf{h}_n^H \mathbf{h}_n \right) \mathbf{p}_T^{(k-1)}. \quad (35)$$

we can find the closed-form optimal transmit beamformer at iteration  $k$ , given by

$$\mathbf{p}_T^{(k)} = \sqrt{2P} \frac{\mathbf{a}^{(k-1)}}{\|\mathbf{a}^{(k-1)}\|}. \quad (38)$$

By iteratively solving the approximate problem through the closed-form solution (38), the proposed SCA algorithm converges to a stationary point of the original problem (29)-(30). Compared with previous methods, the proposed SCA algorithm greatly reduces the computational complexity of transmit beamforming design.

2) *Binary Antenna Coding Design*: Given the fixed transmit beamformer  $\mathbf{p}_T$ ,  $P_{\text{out}}^{\text{DCC}}$  is solely the function of antenna coders  $\mathbf{B}_T$  and  $\mathbf{B}_R$ , so that we can equivalently transform problem (25)-(28) into

$$\max_{\mathbf{B}_T, \mathbf{B}_R} P_{\text{out}}^{\text{DCC}}(\mathbf{B}_T, \mathbf{B}_R) \quad (39)$$

$$\text{s.t. } [\mathbf{B}_T]_{i,j} \in \{0, 1\}, \forall i, j, \quad (40)$$

$$[\mathbf{B}_R]_{i,j} \in \{0, 1\}, \forall i, j. \quad (41)$$

This is an NP-hard binary optimization problem that cannot be solved by gradient-based algorithms but can be solved by heuristic searching methods such as successive exhaustive Boolean optimization (SEBO) [39]. The SEBO algorithm contains two stages: 1) cyclic exhaustive search over each block (of size  $J$ ) of the antenna coders and 2) random bit flips to explore potential better local optimum solutions. Herein, we use a warm-start SEBO where SEBO algorithm is run for multiple rounds and the best solution found in one round serves as the initial point for the next round to enhance the possibility of finding a high-quality solution. Thus, the computational complexity of warm-start SEBO is given by  $\mathcal{O}(I2^JW)$ , where  $I$  denotes the number of iterations and  $W$  denotes the number of rounds for warm-start SEBO. The overall joint transmit beamforming and binary antenna coding design is summarized in Algorithm 1.

### B. Continuous Antenna Coding Optimization with DCC

For continuous antenna coding based on variable reactive loads, we formulate the joint continuous antenna coding and beamforming design problem as

$$\max_{\mathbf{p}_T, \mathbf{B}_T, \mathbf{B}_R} P_{\text{out}}^{\text{DCC}}(\mathbf{p}_T, \mathbf{B}_T, \mathbf{B}_R) \quad (42)$$

$$\text{s.t. } \frac{1}{2} \|\mathbf{p}_T\|^2 \leq P, \quad (43)$$

$$[\mathbf{B}_T]_{i,j} \in [0, 1], \forall i, j, \quad (44)$$

$$[\mathbf{B}_R]_{i,j} \in [0, 1], \forall i, j, \quad (45)$$

where (44) and (45) denote the continuous antenna coder constraints instead. Similarly, the problems (42)-(45) can be decoupled into two sub-problems including transmit beamforming and continuous antenna coding designs.

---

### Algorithm 1 Joint Transmit Beamforming and Binary Antenna Coding Design With DCC

---

- 1: **Initialize:**  $i = 0$ , initial transmit beamformer  $\mathbf{p}_T^{(0)}$ , initial antenna coders  $\mathbf{B}_T^{(0)}$ ,  $\mathbf{B}_R^{(0)}$ , convergence threshold  $\epsilon$ , maximum iterations  $i_{\text{max}}$ ;
- 2: **repeat**
- 3:    $i \leftarrow i + 1$ ;
- 4:   **Update Channel:** Compute the beampspace channel  $\mathbf{H}(\mathbf{B}_T^{(i-1)}, \mathbf{B}_R^{(i-1)}) = \mathbf{W}_R^H(\mathbf{B}_R^{(i-1)})\mathbf{H}_C\mathbf{W}_T(\mathbf{B}_T^{(i-1)})$ ;
- 5:   **Optimize Transmit Beamformer  $\mathbf{p}_T$ :**
- 6:     Fix  $\mathbf{B}_T^{(i-1)}, \mathbf{B}_R^{(i-1)}$ ;
- 7:     Use SCA to solve (29) and (30) and obtain  $\mathbf{p}_T^{(i)}$ ;
- 8:   **Optimize Antenna Coder ( $\mathbf{B}_T, \mathbf{B}_R$ ):**
- 9:     Fix  $\mathbf{p}_T^{(i)}$ ;
- 10:    Obtain  $\mathbf{B}_T^{(i)}, \mathbf{B}_R^{(i)}$  by solving (39)-(41);
- 11: **until** objective change  $< \epsilon$  or  $i = i_{\text{max}}$
- 12: **Output:** Optimal  $\mathbf{p}^* = \mathbf{p}^{(i)}$ ,  $\mathbf{B}_T^* = \mathbf{B}_T^{(i)}$ ,  $\mathbf{B}_R^* = \mathbf{B}_R^{(i)}$ .

---

1) *Transmit Beamforming Design*: Given fixed antenna coders  $\mathbf{B}_T$  and  $\mathbf{B}_R$ , the transmit beamforming design problem remains the same as the problem (29) and (30), which can be solved using the aforementioned SCA algorithm.

2) *Continuous Antenna Coding Design*: Given the fixed transmit beamformer  $\mathbf{p}_T$ , the continuous antenna coding optimization problem is given by

$$\max_{\mathbf{B}_T, \mathbf{B}_R} P_{\text{out}}^{\text{DCC}}(\mathbf{B}_T, \mathbf{B}_R) \quad (46)$$

$$\text{s.t. } [\mathbf{B}_T]_{i,j} \in [0, 1], \forall i, j, \quad (47)$$

$$[\mathbf{B}_R]_{i,j} \in [0, 1], \forall i, j, \quad (48)$$

where the antenna coder  $\mathbf{B}_T$  and  $\mathbf{B}_R$  is linear in the range  $[0, 1]$ . From (5), we have that

$$|x_{T,i,j}| = x_{\text{oc}}[\mathbf{B}_T]_{i,j}, \quad (49)$$

$$|x_{R,i,j}| = x_{\text{oc}}[\mathbf{B}_R]_{i,j}, \quad (50)$$

where  $x_{T,i,j}$  and  $x_{R,i,j}$  denotes the load reactance of the  $i$ th variable reactive load of the  $j$ th transmit and receive pixel antennas, respectively. Note that  $x_{\text{oc}}$  is a very large value to numerically approximate infinity and in theory  $x_{T,i,j}$  and  $x_{R,i,j}$  can have arbitrary value. Therefore, we can equivalently transform the problems (46)-(48) to an unconstrained optimization problem

$$\max_{\mathbf{X}_T, \mathbf{X}_R} P_{\text{out}}^{\text{DCC}}(\mathbf{X}_T, \mathbf{X}_R), \quad (51)$$

where  $\mathbf{X}_T \in \mathbb{R}^{Q \times M}$  and  $\mathbf{X}_R \in \mathbb{R}^{Q \times N}$  are constructed by  $[\mathbf{X}_T]_{i,j} = x_{T,i,j}$  and  $[\mathbf{X}_R]_{i,j} = x_{R,i,j}$  and can have arbitrary value. Therefore, we can use the Quasi-Newton algorithm [40] to solve the problem (51) with convergence to a stationary point. To improve the performance, we run the

**Algorithm 2** Joint Transmit Beamforming and Continuous Antenna Coding Design With DCC

---

```

1: Initialize:  $i = 0$ ,  $\mathbf{p}_T^{(0)}$ ,  $\mathbf{B}_T^{(0)}$ ,  $\mathbf{B}_R^{(0)}$ ,  $\epsilon$ ,  $i_{\max}$ ;
2: repeat
3:    $i \leftarrow i + 1$ ;
4:   Update Channel: Compute the beamspace channel
    $\mathbf{H}(\mathbf{B}_T^{(i-1)}, \mathbf{B}_R^{(i-1)})$ ;
5:   Optimize Transmit Beamformer  $\mathbf{p}_T$ :
6:     Fix  $\mathbf{B}_T^{(i-1)}$ ,  $\mathbf{B}_R^{(i-1)}$ ;
7:     Use SCA to solve (29) and (30) and obtain  $\mathbf{p}_T^{(i)}$ ;
8:   Optimize Antenna Coder ( $\mathbf{B}_T, \mathbf{B}_R$ ):
9:     Fix  $\mathbf{p}_T^{(i)}$ ;
10:    Obtain  $\mathbf{B}_T^{(i)}, \mathbf{B}_R^{(i)}$  by solving (46)-(48);
11: until objective change  $< \epsilon$  or  $i = i_{\max}$ 
12: Output: Optimal  $\mathbf{p}^* = \mathbf{p}^{(i)}$ ,  $\mathbf{B}_T^* = \mathbf{B}_T^{(i)}$ ,  $\mathbf{B}_R^* = \mathbf{B}_R^{(i)}$ .

```

---

Quasi-Newton algorithm 10 times with random initial points in the range  $[-50, 50]$  and subsequently select the best result. The computational complexity of the quasi-Newton method for each iteration is given by  $\mathcal{O}((M + N)^2 Q^2)$  [41]. The overall joint transmit beamforming and continuous antenna coding design is summarized in Algorithm 2.

#### IV. ANTENNA CODING OPTIMIZATION FOR MIMO WPT WITH RF COMBINING

In this section, we formulate and solve the antenna coding optimization problem for MIMO WPT with RF combining (RFC) to maximize the output DC power. An efficient algorithm to jointly optimize antenna coding and transmit and receive beamforming is also proposed.

##### A. Antenna Coding Optimization with RFC

For RFC scheme as shown in Fig. 3, the signals received by the  $N$  receive pixel antennas are first combined with the receive beamformer  $\mathbf{p}_R$  to obtain the combined received signal

$$\tilde{y}(t) = \Re\{\mathbf{p}_R^H \mathbf{H}(\mathbf{B}_T, \mathbf{B}_R) \mathbf{p}_T e^{j\omega_c t}\}, \quad (52)$$

which is then rectified by a single rectifier. Therefore, the output DC voltage is given by

$$v_{\text{out}} = \sum_{i \text{ even}, i \geq 2}^{n_0} \beta_i \zeta_i |\mathbf{p}_R^H \mathbf{H}(\mathbf{B}_T, \mathbf{B}_R) \mathbf{p}_T|^i, \quad (53)$$

which yields the output DC power as  $P_{\text{out}}^{\text{RFC}} = v_{\text{out}}^2 / R_L$ .

We first consider binary antenna coding. We notice that  $P_{\text{out}}^{\text{RFC}}$  monotonically increases with the channel gain  $|\mathbf{p}_R^H \mathbf{H}(\mathbf{B}_T, \mathbf{B}_R) \mathbf{p}_T|^2$ , simplifying the output DC power maximization problem as

$$\max_{\mathbf{p}_T, \mathbf{p}_R, \mathbf{B}_T, \mathbf{B}_R} |\mathbf{p}_R^H \mathbf{H}(\mathbf{B}_T, \mathbf{B}_R) \mathbf{p}_T|^2 \quad (54)$$

$$\text{s.t. } \frac{1}{2} \|\mathbf{p}_T\|^2 \leq P, \quad (55)$$

$$\|\mathbf{p}_R\|^2 \leq 1, \quad (56)$$

$$[\mathbf{B}_T]_{i,j} \in \{0, 1\}, \forall i, j, \quad (57)$$

$$[\mathbf{B}_R]_{i,j} \in \{0, 1\}, \forall i, j. \quad (58)$$

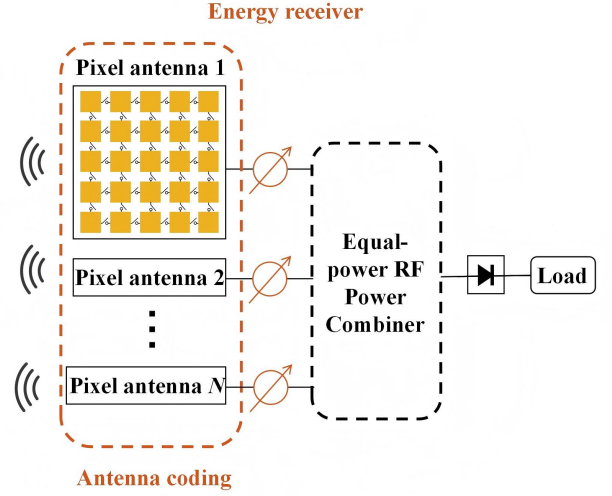


Fig. 4. Schematic of the proposed energy receiver using pixel antennas with analog receive beamforming.

Given arbitrary antenna coders  $\mathbf{B}_T$  and  $\mathbf{B}_R$ , optimal transmit and receive beamforming have closed-form solutions obtained by SVD of  $\mathbf{H}(\mathbf{B}_T, \mathbf{B}_R)$ , written as

$$\mathbf{p}_T^*(\mathbf{B}_T, \mathbf{B}_R) = \mathbf{v}_1(\mathbf{B}_T, \mathbf{B}_R) \sqrt{2P}, \quad (59)$$

$$\mathbf{p}_R^*(\mathbf{B}_T, \mathbf{B}_R) = \mathbf{u}_1(\mathbf{B}_T, \mathbf{B}_R), \quad (60)$$

where  $\mathbf{v}_1(\mathbf{B}_T, \mathbf{B}_R)$  and  $\mathbf{u}_1(\mathbf{B}_T, \mathbf{B}_R)$  denote the right and left singular vectors corresponding to the maximum singular value of  $\mathbf{H}(\mathbf{B}_T, \mathbf{B}_R)$ , denoted as  $\sigma_{\max}(\mathbf{H}(\mathbf{B}_T, \mathbf{B}_R))$ . Substituting (59) and (60) into problems (54)-(58), we have

$$\max_{\mathbf{B}_T, \mathbf{B}_R} 2P |\sigma_{\max}(\mathbf{H}(\mathbf{B}_T, \mathbf{B}_R))|^2 \quad (61)$$

$$\text{s.t. } [\mathbf{B}_T]_{i,j} \in \{0, 1\}, \forall i, j, \quad (62)$$

$$[\mathbf{B}_R]_{i,j} \in \{0, 1\}, \forall i, j, \quad (63)$$

which can be solved by the warm-start SEBO algorithm.

As for the continuous antenna coding, the formulation of the output DC power maximization problem can be easily tailored simply by replacing  $\{0, 1\}$  with  $[0, 1]$  in the constraint (57) and (58), so that it can be solved by the quasi-Newton algorithm similar to problem (46)-(48). For brevity, we omit the details.

##### B. Optimization with Analog Receive Beamforming

The general receive beamforming in RFC scheme requires reconfigurable power combiners to adjust the magnitude of the receiver beamforming weights, which however increases hardware complexity. Therefore, a practical RFC scheme is analog receive beamforming (ABF) utilizing phase shifters with an equal-power combiner as shown in Fig. 4. Using the ABF, we first consider the binary antenna coding and the

output DC power maximization problem formulated as

$$\max_{\mathbf{p}_T, \mathbf{p}_R, \mathbf{B}_T, \mathbf{B}_R} |\mathbf{p}_R^H \mathbf{H}(\mathbf{B}_T, \mathbf{B}_R) \mathbf{p}_T|^2 \quad (64)$$

$$\text{s.t.} \quad \frac{1}{2} \|\mathbf{p}_T\|^2 \leq P, \quad (65)$$

$$|[\mathbf{p}_R]_n| = \frac{1}{\sqrt{N}}, \forall n, \quad (66)$$

$$[\mathbf{B}_T]_{i,j} \in \{0, 1\}, \forall i, j, \quad (67)$$

$$[\mathbf{B}_R]_{i,j} \in \{0, 1\}, \forall i, j, \quad (68)$$

where the constant-modulus constraint (66) complicates the problem. To handle this, we adopt an alternating optimization approach to decouple the analog receive beamforming and antenna coding designs as follows.

1) *Analog Receive Beamforming Design*: Given fixed antenna coders  $\mathbf{B}_T$  and  $\mathbf{B}_R$ , the analog receive beamforming design problem is expressed as

$$\max_{\mathbf{p}_T, \mathbf{p}_R} |\mathbf{p}_R^H \mathbf{H} \mathbf{p}_T|^2 \quad (69)$$

$$\text{s.t.} \quad \frac{1}{2} \|\mathbf{p}_T\|^2 \leq P, \quad (70)$$

$$|[\mathbf{p}_R]_n| = \frac{1}{\sqrt{N}}, \forall n. \quad (71)$$

We notice that for any given  $\mathbf{p}_R$ , the optimal  $\mathbf{p}_T^*$  that maximizes the output DC power is given by the maximum ratio transmission (MRT), i.e.  $\mathbf{p}_T^* = \sqrt{2P} \frac{(\mathbf{p}_R^H \mathbf{H})^H}{\|\mathbf{p}_R^H \mathbf{H}\|}$ . Accordingly, by further introducing an auxiliary variable  $r_0 = \|\mathbf{p}_R^H \mathbf{H}\| > 0$ , the problem (69)-(71) can be equivalently rewritten as

$$\max_{\mathbf{p}_R} r_0^2 \quad (72)$$

$$\text{s.t.} \quad |[\mathbf{p}_R]_n| = \frac{1}{\sqrt{N}}, \forall n. \quad (73)$$

To deal with the non-convex optimization problem (72) and (73), we use SCA to approximate  $r_0^2 = \mathbf{p}_R^H \mathbf{H} \mathbf{H}^H \mathbf{p}_R$  with its first-order Taylor expansion at the  $(k-1)$ th iteration, i.e.

$$r_0^2 \geq 2\Re\{\mathbf{p}_R^{(k-1)H} \mathbf{H} \mathbf{H}^H \mathbf{p}_R\} - \mathbf{p}_R^{(k-1)H} \mathbf{H} \mathbf{H}^H \mathbf{p}_R^{(k-1)}. \quad (74)$$

Ignoring the constant term, we can formulate the approximate problem of (72) and (73) at  $k$ th iteration as

$$\max_{\mathbf{p}_R} \Re\{\mathbf{z}^{(k-1)H} \mathbf{p}_R\} \quad (75)$$

$$\text{s.t.} \quad |[\mathbf{p}_R]_n| = \frac{1}{\sqrt{N}}, \forall n, \quad (76)$$

where  $\mathbf{z}^{(k-1)} = \mathbf{H} \mathbf{H}^H \mathbf{p}_R^{(k-1)}$  is a constant and the closed-form optimal solution can be easily found with

$$\mathbf{p}_R^{(k)} = \frac{1}{\sqrt{N}} e^{j\arg(\mathbf{z}^{(k-1)})}. \quad (77)$$

By iteratively solving the approximate problem through the closed-form solution (77), the SCA algorithm converges to a stationary point of the original problem (69)-(71). The overall analog receive beamforming design is summarized in Algorithm 3.

---

### Algorithm 3 Analog Receive Beamforming Design

---

- 1: **Initialize:**  $k = 0$ ,  $\mathbf{p}_R^{(0)}$ ,  $\epsilon$ ,  $k_{\max}$ ;
- 2: **repeat**
- 3:    $k \leftarrow k + 1$ ;
- 4:   Compute  $\mathbf{z}^{(k-1)} = \mathbf{H} \mathbf{H}^H \mathbf{p}_R^{(k-1)}$ ;
- 5:   Update  $\mathbf{p}_R^{(k)} = \frac{1}{\sqrt{N}} e^{j\arg(\mathbf{z}^{(k-1)})}$ ;
- 6:   **until**  $\|\mathbf{p}_R^{(k)} - \mathbf{p}_R^{(k-1)}\| / \|\mathbf{p}_R^{(k)}\| < \epsilon$  or  $k = k_{\max}$
- 7: Set  $\mathbf{p}_T^{(k)} = \sqrt{2P} \frac{(\mathbf{p}_R^{(k)H} \mathbf{H})^H}{\|\mathbf{p}_R^{(k)H} \mathbf{H}\|}$ ;
- 8: **Output:**  $\mathbf{p}_T^* = \mathbf{p}_T^{(k)}$ ,  $\mathbf{p}_R^* = \mathbf{p}_R^{(k)}$ .

---

2) *Antenna Coding Design*: Given fixed beamformers  $\mathbf{p}_T$  and  $\mathbf{p}_R$ , the binary antenna coding design problem can be formulated as

$$\max_{\mathbf{B}_T, \mathbf{B}_R} |\mathbf{p}_R^H \mathbf{H}(\mathbf{B}_T, \mathbf{B}_R) \mathbf{p}_T|^2 \quad (78)$$

$$\text{s.t.} \quad [\mathbf{B}_T]_{i,j} \in \{0, 1\}, \forall i, j, \quad (79)$$

$$[\mathbf{B}_R]_{i,j} \in \{0, 1\}, \forall i, j, \quad (80)$$

which can be solved by the warm-start SEBO algorithm, with  $\mathbf{p}_T$  given by MRT and fixed  $\mathbf{p}_R$ .

By alternatively optimizing the transmit and receiving beamforming and antenna coding designs, the output DC power with ABF and binary antenna coding can be maximized. Further, the output DC power maximization with ABF and continuous antenna coding can be easily tailored by replacing  $\{0, 1\}$  with  $[0, 1]$  in the constraint (67) and (68), and solved by the quasi-Newton algorithm. For brevity, we omit the details.

## V. CODEBOOK-BASED ANTENNA CODING DESIGN

To reduce the computational complexity of binary antenna coding optimization, we propose a codebook-based antenna coding design strategy, which is based on K-means clustering tailored for output DC power maximization problem for the proposed MIMO WPT system.

### A. Problem Formulation

A codebook design has been demonstrated in [32] for maximizing the average channel gain of SISO pixel antenna systems. It was based on the generalized Lloyd algorithm (GLA), where the training channel partitions and antenna coder centroids are alternatively optimized until convergence. However, this method lacks consideration for MIMO WPT configurations and the specific optimization objective beyond channel gain. Hence, we aim to propose a scenario-oriented codebook design method for the output DC power maximization problem with DCC and RFC, respectively.

To this end, we consider a codebook containing  $D$  different antenna coders as  $\mathcal{C} \triangleq \{\mathbf{c}_1, \dots, \mathbf{c}_D\}$ , where  $\mathbf{c}_d \in \mathbb{R}^{Q \times 1}$  is the  $d$ th antenna coder, also referred to as a codeword. Taking the antenna coding optimization for MIMO WPT with RFC as

an example, the output DC power maximization problem with antenna coders selected from the codebook  $\mathcal{C}$  is written as

$$\max_{\mathbf{B}_T, \mathbf{B}_R} |\sigma_{\max}(\mathbf{H}(\mathbf{B}_T, \mathbf{B}_R))|^2 \quad (81)$$

$$\text{s.t. } [\mathbf{B}_T]_{:,m} \in \mathcal{C}, \forall m, \quad (82)$$

$$[\mathbf{B}_R]_{:,n} \in \mathcal{C}, \forall n, \quad (83)$$

where the optimal transmit and receive beamformers (59) and (60) are implicitly utilized. However, to obtain the optimal antenna coders  $\mathbf{B}_T^*$  and  $\mathbf{B}_R^*$  from the codebook, we need to first design a good codebook to maximize the average output DC power of the MIMO WPT system, written as

$$\max_{\mathcal{C}} \mathcal{E} \left\{ |\sigma_{\max}(\mathbf{H}(\mathbf{B}_T^*, \mathbf{B}_R^*))|^2 \right\} \quad (84)$$

$$\text{s.t. } [\mathbf{c}_d]_q \in \{0, 1\}, \forall d, q, \quad (85)$$

$$\mathbf{B}_T^*, \mathbf{B}_R^* \text{ solves (81) - (83),} \quad (86)$$

which can be regarded as an upper-level problem of (81)-(83). To solve the nested optimization problems, we adopt a two-stage process: 1) the offline codebook training stage, which provides a codebook design for antenna coding, and 2) the online deployment stage, which searches for optimal antenna coders among the pre-designed codebook.

### B. Offline Codebook Training

For the offline codebook training problem (84)-(86), we assume a training set consisting of  $N_0$  channel realizations, following the same distribution of  $\mathbf{H}_C$

$$\mathcal{H}_0 \triangleq \{\mathbf{H}_C^{[1]}, \mathbf{H}_C^{[2]}, \dots, \mathbf{H}_C^{[N_0]}\}. \quad (87)$$

Given the  $N_0$  training channels, we first solve the output DC power maximization problem with RFC for each training channel realization

$$\max_{\mathbf{B}_T, \mathbf{B}_R} \left| \sigma_{\max} \left( \mathbf{W}_R^H (\mathbf{B}_R) \mathbf{H}_C^{[n_0]} \mathbf{W}_T (\mathbf{B}_T) \right) \right|^2 \quad (88)$$

$$\text{s.t. } [\mathbf{B}_T]_{i,j} \in \{0, 1\}, \forall i, j, \quad (89)$$

$$[\mathbf{B}_R]_{i,j} \in \{0, 1\}, \forall i, j, \quad (90)$$

where the warm-start SEBO algorithm can be used to find the optimal antenna coders denoted as  $\mathbf{B}_T^{[n_0]}$  and  $\mathbf{B}_R^{[n_0]} \forall n_0$ . To facilitate the codebook design shared by all pixel antennas at ET and ER, we collect the antenna coders for each transmit and receive pixel antenna into a set denoted as

$$\mathcal{B}^{[n_0]} = \left\{ [\mathbf{B}_T^{[n_0]}]_{:,m} \mid \forall m \right\} \cup \left\{ [\mathbf{B}_R^{[n_0]}]_{:,n} \mid \forall n \right\}, \quad (91)$$

which has  $M + N$  elements. Furthermore, we collect  $\mathcal{B}^{[n_0]} \forall n_0$  into a set with  $L = (M + N)N_0$  elements, that is

$$\mathcal{B} = \bigcup_{\forall n_0} \mathcal{B}^{[n_0]} = \{\bar{\mathbf{b}}_1, \bar{\mathbf{b}}_2, \dots, \bar{\mathbf{b}}_L\}, \quad (92)$$

where  $\bar{\mathbf{b}}_l$  denotes the  $l$ th element (antenna coder). As a result, we can design the codebook  $\mathcal{C}$  by optimizing its  $D$  codewords to approximate the set  $\mathcal{B}$ . This is similar to a vector quantization problem, where the average distortion between the antenna coders in the set  $\mathcal{B}$  and the codewords

is minimized in terms of Euclidean distance (i.e. Hamming distance for binary vectors), written as

$$\{\mathbf{c}_1^*, \dots, \mathbf{c}_D^*\} = \underset{[\mathbf{c}_d]_q \in \{0, 1\}, \forall d, q}{\operatorname{argmin}} \frac{1}{L} \sum_{l=1}^L \|\bar{\mathbf{b}}_l - \mathbf{c}_d\|, \quad (93)$$

where  $\mathbf{c}_1^*, \dots, \mathbf{c}_D^*$  denotes the optimized codewords.

To solve the problem (93), which can be regarded as a K-means clustering problem in a multi-dimensional feature space of size  $Q$ , we follow an alternating optimization strategy: 1) the antenna coder is individually assigned to their nearest codewords as cluster centers in the current codebook in terms of Euclidean distance; 2) the cluster centers are updated to minimize the average distortion between it and the assigned antenna coders. To characterize the antenna coder assignment given a fixed codebook  $\mathcal{C}$ , we introduce binary assignment variables  $r_{l,d} \in \{0, 1\}$ ,  $l = 1, \dots, L$ ,  $d = 1, \dots, D$ , which equals 1 only when the  $l$ th antenna coder  $\bar{\mathbf{b}}_l$  is assigned to the  $d$ th codeword  $\mathbf{c}_d$ . Therefore, problem (93) can be equivalently rewritten as

$$\{\mathbf{c}_1^*, \dots, \mathbf{c}_D^*\} = \underset{[\mathbf{c}_d]_q, r_{l,d} \in \{0, 1\}}{\operatorname{argmin}} \sum_{l=1}^L \sum_{d=1}^D r_{l,d} \|\bar{\mathbf{b}}_l - \mathbf{c}_d\|, \quad (94)$$

To solve (94), the two alternating steps are detailed as below.

1) *Antenna Coder Assignment*: Given fixed codewords  $\{\mathbf{c}_1^{(k-1)}, \dots, \mathbf{c}_D^{(k-1)}\}$  as cluster centers, we optimize the assignment variables  $r_{l,d}^{(k)} \forall l, d$  at  $k$ th iteration by assigning  $\bar{\mathbf{b}}_l$  to the nearest cluster center, expressed as

$$r_{l,d}^{(k)} = \begin{cases} 1 & \text{if } d = \operatorname{argmin}_i \|\bar{\mathbf{b}}_l - \mathbf{c}_i^{(k-1)}\|, \\ 0 & \text{else} \end{cases}, \quad \forall l, d, \quad (95)$$

where  $\mathbf{c}_i^{(k-1)}$  is the  $i$ th codeword (cluster center) optimized at the  $(k-1)$ th iteration.

2) *Cluster Center Update*: Given fixed assignment variables  $r_{l,d}^{(k)} \forall l, d$ , we can update the cluster centers at  $k$ th iteration to minimize the average distortion between the cluster centers and the assigned antenna coders

$$\{\mathbf{c}_1^{(k)}, \dots, \mathbf{c}_D^{(k)}\} = \underset{[\mathbf{c}_d^{(k)}]_q \in \{0, 1\}}{\operatorname{argmin}} \sum_{l=1}^L \sum_{d=1}^D r_{l,d}^{(k)} \|\bar{\mathbf{b}}_l - \mathbf{c}_d^{(k)}\|, \quad (96)$$

which is a binary optimization problem and can be solved by the warm-start SEBO algorithm.

By alternatively optimizing the antenna coder assignment (95) and cluster center update (96), the average distortion decreases over each iteration until the codebook design converges. The overall offline codebook training is summarized in Algorithm 4. It can be applied to different combining schemes and beamforming strategies, and only requires an update to the objective function to obtain antenna coder  $\bar{\mathbf{b}}_l \forall l$ .

### C. Online Codebook Deployment

Once the offline codebook  $\mathcal{C}$  is obtained, the antenna coders are optimized during the online deployment stage of (81)-(83) with the CSI of  $\mathbf{H}_C$ . This can be done by iteratively searching the best codeword for each pixel antenna while fixing the codewords for other pixel antennas until convergence, which is

**Algorithm 4** Offline Codebook Training for Antenna Coding

- 1: **Input:** Training channel set  $\mathcal{H}_0 = \{\mathbf{H}_C^{[1]}, \dots, \mathbf{H}_C^{[N_0]}\}$ , codebook size  $D$ ;
- 2: **Initialize:**  $k = 0$ ,  $\mathcal{C}^{(0)} = \{\mathbf{c}_1^{(0)}, \dots, \mathbf{c}_D^{(0)}\}$ ,  $\epsilon$ ,  $k_{\max}$ ;
- 3: Obtain optimal antenna coder set  $\mathcal{B} = \{\bar{\mathbf{b}}_1, \dots, \bar{\mathbf{b}}_L\}$  via warm-start SEBO and (91)(92);
- 4: **repeat**
- 5:      $k \leftarrow k + 1$ ;
- 6:     **Antenna Coder Assignment:**
- 7:     Fix  $\{\mathbf{c}_1^{(k-1)}, \dots, \mathbf{c}_D^{(k-1)}\}$ ;
- 8:     Optimize  $\{r_{ld}^{(k)}, \forall l, d\}$  by (95);
- 9:     **Cluster Center Update:**
- 10:     Fix  $\{r_{ld}^{(k)}, \forall l, d\}$ ;
- 11:     Update codewords  $\{\mathbf{c}_1^{(k)}, \dots, \mathbf{c}_D^{(k)}\}$  by solving (96) ;
- 12: **until** Objective change  $< \epsilon$  or  $k = k_{\max}$
- 13: **Output:** Optimized codebook  $\mathcal{C}^* = \{\mathbf{c}_1^{(k)}, \dots, \mathbf{c}_D^{(k)}\}$ .

similar to the block coordinate descent (BCD) method. During the online deployment stage, only  $(M + N)D$  searches are required for each iteration, which is much more computationally efficient than the warm-start SEBO optimization.

## VI. PERFORMANCE EVALUATION

In this section, we evaluate the performance of MIMO WPT systems with DCC and RFC with the proposed binary and continuous antenna coding designs using pixel antennas. The codebook-based antenna coding design is also evaluated.

### A. Simulation Setup and Pixel Antenna

A rich scattering environment is considered with a 2-D uniform power angular spectrum and  $K = 72$  sampled spatial angles. The pixel antennas deployed at ER and ET are identical but are reconfigured with different antenna coders. Following the setting in [32], we consider a  $0.5\lambda \times 0.5\lambda$  pixel antenna operating at 2.4 GHz (wavelength  $\lambda = 125$  mm) with one antenna port and  $Q = 39$  pixel ports. Obtaining the impedance matrix  $\mathbf{Z}$  and open-circuit radiation pattern matrix  $\mathbf{E}_{oc}$  from CST Studio Suite, we determine the EADoF  $N_{\text{eff}}$  by calculating the dominant singular values of  $\mathbf{E}_{oc}$  that accounts for more than 99.8% of total radiated power. This gives  $N_{\text{eff}} = 7$  and the corresponding orthogonal basis patterns are shown in Fig. 5.

Assuming a multipath Rayleigh fading environment, the entries of channel matrix  $\mathbf{H}_C$  are modeled as i.i.d complex Gaussian random variables, i.e.  $[\mathbf{H}_C]_{i,j} \sim \mathcal{CN}(0, 1) \forall i, j$ . We assume 36 dBm transmit power and 66 dB path loss. The rectenna model parameters are given as  $R_{\text{ant}} = 50\Omega$ ,  $R_L = 5k\Omega$ ,  $I_d = 1.05$ ,  $v_t = 25\text{mV}$ . In the warm-start SEBO, the block size is  $J = 10$  and the number of rounds is  $W = 20$ . The Monte Carlo method with 1000 channel realizations is utilized to obtain the average output DC power.

### B. MIMO WPT Performance with Antenna Coding

We first evaluate the performance of the proposed MIMO WPT system utilizing pixel antennas with binary antenna

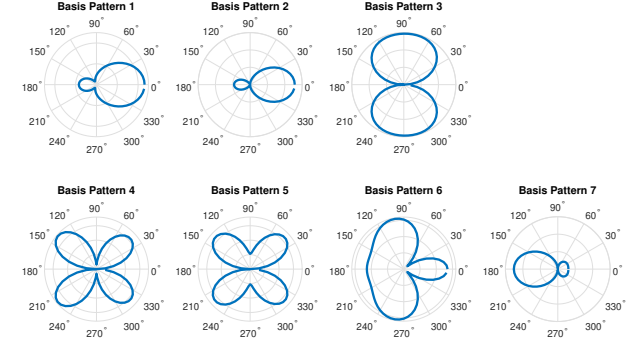


Fig. 5. The orthogonal basis patterns provided by the pixel antenna in [32].

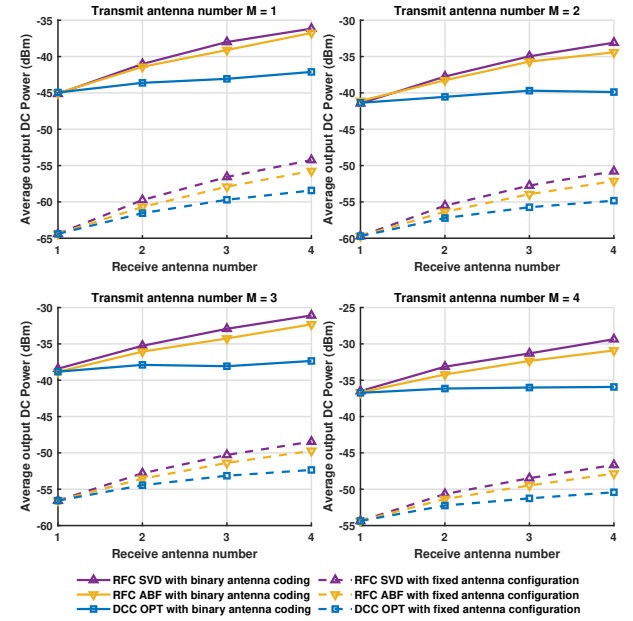


Fig. 6. Average output DC power versus receive antenna number for different transmit antenna numbers, with binary antenna coding and with fixed antenna configuration, under different DC and RF combining schemes.

coding under different DC and RF combining schemes, including 1) the DCC with optimized (OPT) beamforming, 2) the RFC with SVD beamforming, and 3) the RFC with ABF. In addition, we also compare with the conventional MIMO WPT system utilizing antennas with fixed configuration under different DC and RF combining schemes.

Fig. 6 displays the average output DC power of the MIMO WPT system versus the receive antenna number for different transmit antenna numbers, with binary antenna coding and with fixed antenna configuration, under different DC and RF combining schemes. We can make the following observations.

*First*, with the increase of transmit/receive antenna numbers, the output DC power of MIMO WPT systems with both binary antenna coding and fixed antenna configuration can be increased, which shows that using pixel antennas to construct MIMO WPT systems will not affect exploiting the spatial diversity for MIMO system.

*Second*, the output DC power optimized with binary an-

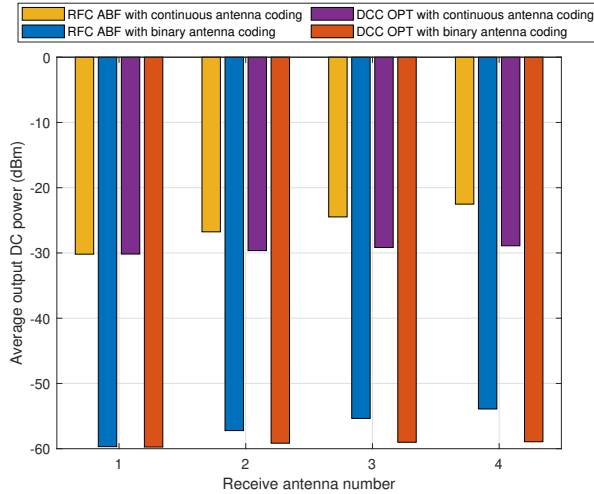


Fig. 7. Average output DC power versus receive antenna number with binary and continuous antenna coding.

tenna coding utilizing pixel antennas (solid lines) significantly outperforms that with conventional fixed antenna configuration (dashed lines) by more than 15 dB for any transmit/receive antenna number. The performance gap becomes more prominent with increased transmit/receive antennas. This enhancement is achieved through additional degrees of freedom introduced by antenna coding, where the radiation patterns are flexibly re-configured to adapt to the channel matrix, leading to coherent adding of different multiple paths with different AoA and AoD in the propagation environment.

Third, RFC schemes obtain higher output DC power than DCC schemes, with both binary antenna coding and fixed antenna configuration. This is because the receive beamforming in RF combining can leverage the rectenna nonlinearity more efficiently than DCC. In addition, it also demonstrates that the extra degrees of freedom provided by pixel antennas can synergize with exploiting the rectenna nonlinearity to jointly enhance the output DC power in MIMO WPT systems.

Fourth, with the constant-modulus constraint of the phase shifter, there is some performance degradation introduced by the analog receive beamforming compared with RFC, with both binary antenna coding and fixed antenna configuration, but the hardware complexity can be effectively reduced as the reconfigurable power combiner is not required.

We also evaluate the performance of the proposed MIMO WPT system with the continuous antenna coding design in comparison with the binary antenna coding design. The average output DC power versus receive antenna number for  $M = 4$  transmit antennas, with binary and continuous antenna coding, is shown in Fig. 7. We can observe that the average output DC power with continuous antenna coding outperforms that with binary antenna coding by more than 6 dB for both RFC and DCC schemes. This can be explained by the fact that the load reactance of continuous antenna coding is continuous from zero to infinity while the load reactance of binary antenna coding is either zero or infinity, which is

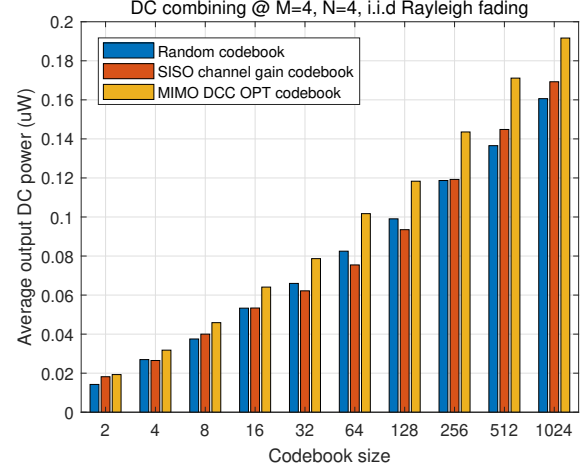


Fig. 8. Average output DC power versus codebook size with codebook-based antenna coding using DCC.

tighter during antenna coding optimization. Hence, continuous antenna coding provides an upper bound of average output DC power of MIMO WPT system using pixel antennas.

Overall, we have shown that using pixel antennas with binary and continuous antenna coding is very beneficial for enhancing the output DC power of MIMO WPT systems due to the extra degrees of freedom, especially when jointly exploiting the rectenna nonlinearity to further boost the output DC power.

### C. MIMO WPT Performance with Codebook Design

We next evaluate the performance of the proposed MIMO WPT system using pixel antennas with codebook-based antenna coding design. For the offline codebook design, we use the  $2 \times 2$  MIMO configuration, which takes multiple pixel antennas into consideration while maintaining an acceptable complexity, and  $N_0 = 15000$  channel realizations for training. We evaluate the proposed MIMO DCC/RFC OPT codebook, which is designed by Algorithm 4 with the antenna coder training set  $\mathcal{B}$  obtained by the proposed DCC/RFC with SVD beamforming for brevity. This is compared with benchmarks including: 1) Random codebook, designed by random binary variable; 2) SISO channel gain codebook, designed in [32] to maximize the channel gain in SISO system.

Fig. 8 and Fig. 9 display the average output DC power of  $4 \times 4$  MIMO WPT system versus the codebook size with codebook-based antenna coding using DCC and RFC, deployed online with OPT and SVD beamforming, respectively. From Fig. 8 and Fig. 9, we make the following observations.

First, the average output DC power of the MIMO WPT system with codebook-based antenna coding increases with the codebook size. This is because increasing the codebook size enlarges the searching space for antenna coding optimization. Therefore, the pixel antennas can provide higher reconfigurability with more diverse radiation patterns to adapt to the channel to enhance the MIMO WPT system. Moreover, as the codebook size increases, the average output DC power optimized with codebook gradually approaches that optimized

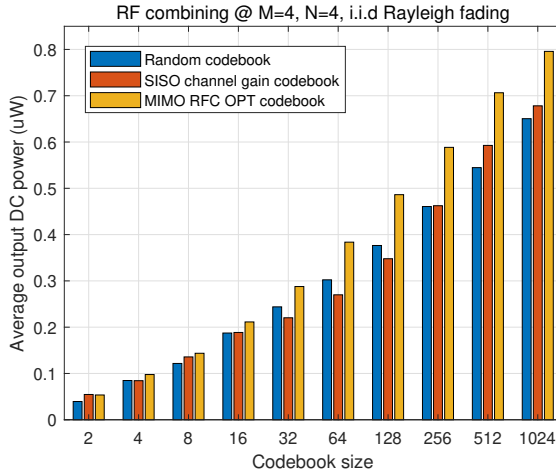


Fig. 9. Average output DC power versus codebook size with codebook-based antenna coding using RFC.

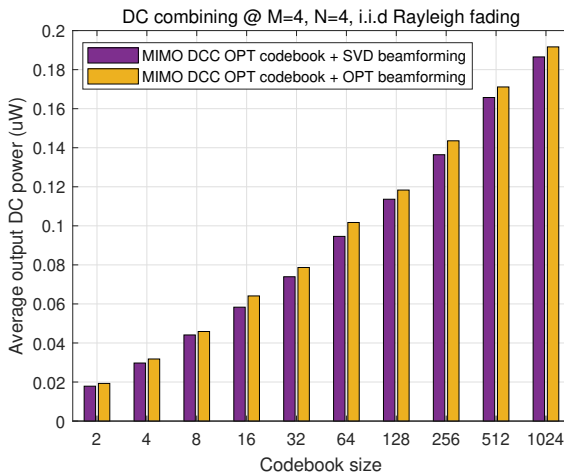


Fig. 10. Average output DC power versus codebook size with codebook-based antenna coding using DCC with different beamforming schemes.

with SEBO. For example, the proposed codebook-based antenna coding design can achieve 61% of the output DC power optimized with SEBO for both RFC and DCC schemes, but with significantly reduced computational complexity.

Second, the proposed MIMO DCC/RFC OPT codebook outperforms the random codebook and SISO channel gain codebook for all cases. For example, in Fig. 8, the proposed codebook design can improve the output DC power by up to 35% compared with the random codebook. In Fig. 9, the proposed codebook design can achieve up to 40% performance enhancement compared with the SISO channel gain codebook. Such improvement is because the proposed codebook design is optimized with considering the MIMO WPT configuration and the objective of maximizing output DC power, instead of the SISO channel gain. Therefore, it demonstrates the benefits of the proposed method to design efficient codebook for antenna coding for MIMO WPT system.

To investigate the impact of rectenna nonlinearity in the proposed pixel antenna MIMO WPT system, as shown in Fig. 10, we consider the output DC power optimized by the

MIMO DCC OPT codebook and the aforementioned OPT beamforming. This provides a comparison with that optimized by the MIMO DCC OPT codebook and the SVD beamforming where the transmit beamformer is given by  $\mathbf{p}_T = \mathbf{v}_1 \sqrt{2P}$  using SVD for each channel realization that is optimal for linear rectenna model. From Fig. 10, we can find that the output DC power with OPT beamforming is higher than that with SVD beamforming. In other words, the MIMO DCC OPT codebook with SVD beamforming is suboptimal as it overlooks the important characteristics of rectenna nonlinearity in WPT. Hence, rectenna nonlinearity should also be properly leveraged, together with antenna coding, to enhance the output DC power of MIMO WPT systems utilizing pixel antennas.

Overall, the proposed codebook design achieves a good tradeoff between output DC power and computational complexity, demonstrating its benefit for antenna coding design for MIMO WPT systems.

## VII. CONCLUSIONS

In this work, we propose a novel antenna coding design for pixel antenna empowered MIMO WPT systems to address the low power transfer efficiency limitation. First, we introduce the antenna coding scheme and beampoint channel model to demonstrate additional degrees of freedom provided by pixel antennas. Then, we formulate the DC power maximization problem with DC and RF combining schemes and propose joint antenna coding and beamforming design methods, where both binary and continuous antenna coders are considered. Efficient SCA algorithms are proposed for beamforming designs with closed-form solution updates. To reduce the computational complexity of binary antenna coding optimization, an efficient codebook design method based on K-means clustering is proposed for MIMO WPT systems.

We also evaluate the proposed pixel antenna empowered MIMO WPT system designs with antenna coding. By jointly exploiting gains from antenna coding, beamforming, and rectenna nonlinearity, a significant 15 dB enhancement in average output DC power can be achieved by binary antenna coding, compared with conventional MIMO WPT systems with fixed antenna configuration. Moreover, the performance can be further improved by another 6 dB with continuous antenna coding. The proposed codebook for antenna coding also outperforms a random codebook and the previous design by up to 40%. It also achieves 61% of the output DC power optimized with SEBO binary optimization, but with much lower computational complexity. All these results have demonstrated the potential of leveraging antenna coding utilizing pixel antennas to enhance WPT systems.

## REFERENCES

- [1] B. Clerckx, J. Kim, K. W. Choi, and D. I. Kim, "Foundations of wireless information and power transfer: Theory, prototypes, and experiments," *Proc. IEEE*, vol. 110, no. 1, pp. 8–30, 2022.
- [2] M. Wagih, A. S. Weddell, and S. Beeby, "Rectennas for radio-frequency energy harvesting and wireless power transfer: A review of antenna design [antenna applications corner]," *IEEE Antennas Propag. Mag.*, vol. 62, no. 5, pp. 95–107, 2020.

- [3] M. A. Ullah, R. Keshavarz, M. Abolhasan, J. Lipman, K. P. Esselle, and N. Shariati, "A review on antenna technologies for ambient RF energy harvesting and wireless power transfer: Designs, challenges and applications," *IEEE Access*, vol. 10, pp. 17 231–17 267, 2022.
- [4] S. Shen, Y. Zhang, C.-Y. Chiu, and R. Murch, "An ambient RF energy harvesting system where the number of antenna ports is dependent on frequency," *IEEE Trans. Microw. Theory Tech.*, vol. 67, no. 9, pp. 3821–3832, 2019.
- [5] S. Shen, C.-Y. Chiu, and R. D. Murch, "A dual-port triple-band L-probe microstrip patch rectenna for ambient RF energy harvesting," *IEEE Trans. Antennas Wireless Propag. Lett.*, vol. 16, pp. 3071–3074, 2017.
- [6] Shen, Shanpu and Chiu, Chi-Yuk and Murch, Ross D, "Multiport pixel rectenna for ambient RF energy harvesting," *IEEE Trans. Antennas Propag.*, vol. 66, no. 2, pp. 644–656, 2017.
- [7] S. Shen, Y. Zhang, C.-Y. Chiu, and R. Murch, "Directional multiport ambient RF energy-harvesting system for the Internet of Things," *IEEE Internet Things J.*, vol. 8, no. 7, pp. 5850–5865, 2020.
- [8] B. Clerckx, R. Zhang, R. Schober, D. W. K. Ng, D. I. Kim, and H. V. Poor, "Fundamentals of wireless information and power transfer: From RF energy harvester models to signal and system designs," *IEEE J. Sel. Areas Commun.*, vol. 37, no. 1, pp. 4–33, 2018.
- [9] Y. Zeng, B. Clerckx, and R. Zhang, "Communications and signals design for wireless power transmission," *IEEE Trans. Commun.*, vol. 65, no. 5, pp. 2264–2290, 2017.
- [10] B. Clerckx and E. Bayguzina, "Waveform design for wireless power transfer," *IEEE Trans. Signal Process.*, vol. 64, no. 23, pp. 6313–6328, 2016.
- [11] S. Shen and B. Clerckx, "Beamforming optimization for MIMO wireless power transfer with nonlinear energy harvesting: RF combining versus DC combining," *IEEE Trans. Wireless Commun.*, vol. 20, no. 1, pp. 199–213, 2020.
- [12] S. Shen and B. Clerckx, "Joint waveform and beamforming optimization for MIMO wireless power transfer," *IEEE Trans. Commun.*, vol. 69, no. 8, pp. 5441–5455, 2021.
- [13] Y. Huang and B. Clerckx, "Large-scale multiantenna multisine wireless power transfer," *IEEE Trans. Signal Process.*, vol. 65, no. 21, pp. 5812–5827, 2017.
- [14] M. R. V. Moghadam, Y. Zeng, and R. Zhang, "Waveform optimization for radio-frequency wireless power transfer," in *2017 IEEE 18th International Workshop on Signal Processing Advances in Wireless Communications (SPAWC)*. IEEE, 2017, pp. 1–6.
- [15] B. A. Cetiner, H. Jafarkhani, J.-Y. Qian, H. J. Yoo, A. Grau, and F. De Flaviis, "Multifunctional reconfigurable MEMS integrated antennas for adaptive MIMO systems," *IEEE Commun. Mag.*, vol. 42, no. 12, pp. 62–70, 2004.
- [16] Y. Zhang, Z. Han, S. Tang, S. Shen, C.-Y. Chiu, and R. Murch, "A highly pattern-reconfigurable planar antenna with 360° single-and multi-beam steering," *IEEE Trans. Antennas Propag.*, vol. 70, no. 8, pp. 6490–6504, 2022.
- [17] Y. Zhang, S. Tang, Z. Han, J. Rao, S. Shen, M. Li, C.-Y. Chiu, and R. Murch, "A low-profile microstrip vertically polarized endfire antenna with 360° beam-scanning and high beam-shaping capability," *IEEE Trans. Antennas Propag.*, vol. 70, no. 9, pp. 7691–7702, 2022.
- [18] J. Rao, Y. Zhang, S. Tang, Z. Li, S. Shen, C.-Y. Chiu, and R. Murch, "A novel reconfigurable intelligent surface for wide-angle passive beam-forming," *IEEE Trans. Microw. Theory Tech.*, vol. 70, no. 12, pp. 5427–5439, 2022.
- [19] C.-Y. Chiu, J. Li, S. Song, and R. D. Murch, "Frequency-reconfigurable pixel slot antenna," *IEEE Trans. Antennas Propag.*, vol. 60, no. 10, pp. 4921–4924, 2012.
- [20] S. Song and R. D. Murch, "An efficient approach for optimizing frequency reconfigurable pixel antennas using genetic algorithms," *IEEE Trans. Antennas Propag.*, vol. 62, no. 2, pp. 609–620, 2014.
- [21] W. Zheng, Y. Yang, and H. Li, "Design of polarization reconfigurable pixel antennas with optimized PIN-diode implementation," *IEEE Trans. Antennas Propag.*, 2024.
- [22] K. K. Wong, A. Shojaeifard, K.-F. Tong, and Y. Zhang, "Performance limits of fluid antenna systems," *IEEE Commun. Lett.*, vol. 24, no. 11, pp. 2469–2472, 2020.
- [23] K.-K. Wong, A. Shojaeifard, K.-F. Tong, and Y. Zhang, "Fluid antenna systems," *IEEE Trans. Wireless Commun.*, vol. 20, no. 3, pp. 1950–1962, 2020.
- [24] C. Psomas, G. M. Kraidy, K.-K. Wong, and I. Krikidis, "On the diversity and coded modulation design of fluid antenna systems," *IEEE Trans. Wireless Commun.*, vol. 23, no. 3, pp. 2082–2096, 2023.
- [25] L. Zhu, W. Ma, and R. Zhang, "Modeling and performance analysis for movable antenna enabled wireless communications," *IEEE Trans. Wireless Commun.*, vol. 23, no. 6, pp. 6234–6250, 2023.
- [26] J. Zhang, J. Rao, Z. Li, Z. Ming, C.-Y. Chiu, K.-K. Wong, K.-F. Tong, and R. Murch, "A novel pixel-based reconfigurable antenna applied in fluid antenna systems with high switching speed," *IEEE Open J. Antennas Propag.*, 2024.
- [27] K.-K. Wong, C. Wang, S. Shen, C.-B. Chae, and R. Murch, "Reconfigurable pixel antennas meet fluid antenna systems: A paradigm shift to electromagnetic signal and information processing," *IEEE Wireless Communications*, pp. 1–8, 2025.
- [28] K.-K. Wong, K.-F. Tong, Y. Chen, and Y. Zhang, "Fast fluid antenna multiple access enabling massive connectivity," *IEEE Commun. Lett.*, vol. 27, no. 2, pp. 711–715, 2022.
- [29] F. R. Ghadi, M. Kaveh, K.-K. Wong, D. Martin, R. Jantti, and Z. Yan, "Physical layer security in FAS-aided wireless powered NOMA systems," *arXiv preprint arXiv:2501.09106*, 2025.
- [30] L. Zhou, J. Yao, T. Wu, M. Jin, C. Yuen, and F. Adachi, "Fluid antenna-assisted simultaneous wireless information and power transfer systems," *IEEE Trans. Veh. Technol.*, 2025.
- [31] X. Lin, Y. Zhao, H. Yang, J. Hu, and K.-K. Wong, "Fluid antenna multiple access assisted integrated data and energy transfer: Outage and multiplexing gain analysis," *IEEE Trans. Wireless Commun.*, 2025.
- [32] S. Shen, K.-K. Wong, and R. Murch, "Antenna coding empowered by pixel antennas," *IEEE Trans. Commun.*, pp. 1–1, 2025.
- [33] H. Li and S. Shen, "Antenna coding design based on pixel antennas for multi-user MISO systems," in *2025 IEEE 26th International Workshop on Signal Processing and Artificial Intelligence for Wireless Communications (SPAWC)*. IEEE, 2025, pp. 1–5.
- [34] Y. Chen, S. Shen, T. Qiao, H. Li, J. Qian, and R. Murch, "Antenna coding optimization based on pixel antennas for MIMO wireless power transfer with DC combining," in *2025 IEEE Globecom Workshops (GC Wkshps): Workshop on Fluid Antenna System (FAS) for 6G (GC Wkshps 2025-FAS 6G)*, Taipei, Taiwan, Dec. 2025, p. 5.77.
- [35] D. H. Johnson and D. E. Dudgeon, *Array signal processing: concepts and techniques*. Simon & Schuster, Inc., 1992.
- [36] Z. Han, S. Shen, Y. Zhang, S. Tang, C.-Y. Chiu, and R. Murch, "Using loaded N-port structures to achieve the continuous-space electromagnetic channel capacity bound," *IEEE Trans. Wireless Commun.*, vol. 22, no. 11, pp. 7592–7605, 2023.
- [37] C. Zhang, S. Shen, Z. Han, and R. Murch, "Analog beamforming using ESPAR for single-RF precoding systems," *IEEE Trans. Wireless Commun.*, vol. 22, no. 7, pp. 4387–4400, 2022.
- [38] C.-W. Liu, H.-H. Lee, P.-C. Liao, Y.-L. Chen, M.-J. Chung, and P.-H. Chen, "Dual-source energy-harvesting interface with cycle-by-cycle source tracking and adaptive peak-inductor-current control," *IEEE J. Solid-State Circuits*, vol. 53, no. 10, pp. 2741–2750, 2018.
- [39] S. Shen, Y. Sun, S. Song, D. P. Palomar, and R. D. Murch, "Successive boolean optimization of planar pixel antennas," *IEEE Trans. Antennas Propag.*, vol. 65, no. 2, pp. 920–925, 2016.
- [40] P. E. Gill and W. Murray, "Quasi-Newton methods for unconstrained optimization," *IMA J. Appl. Math.*, vol. 9, no. 1, pp. 91–108, 1972.
- [41] M. J. Powell, "Updating conjugate directions by the BFGS formula," *Math. Program.*, vol. 38, pp. 29–46, 1987.